Quantum Field Theory of Inelastic Diffraction. III. Dynamical Theory*

C. B. Duke† and U. Landman†
Department of Physics, Materials Research Laboratory and Coordinated Science Laboratory, University of Illinois, Urbana, Illinois 61801
(Received 27 March 1972)

Using our previously developed quantum field theory of electron-solid scattering, we construct a dynamical (i.e., multiple-scattering) theory of inelastic-low-energy-electron diffraction (ILEED) in which the incident electron scatters elastically from the lattice potential an arbitrary number of times both "before" and "after" an inelastic loss. We consider the two cases in which the electron's energy loss is caused by the excitation of a single surface or bulk plasmon. Three types of scattering processes occur: loss before (multiple elastic) diffraction, diffraction before loss, and diffraction before and after loss. The summation over all multiple-elastic-scattering events introduces renormalized elastic-diffraction vertices relative to those used in the kinematical "two-step" model described in Paper II of this series. In the cases of loss before diffraction and diffraction before loss, this renormalization is the only consequence of multiple elastic scattering. The processes of diffraction both before and after loss occur only in the dynamical theory and, consequently, are strictly multiple-scattering phenomena. Explicit expressions for the cross sections, suitable for numerical evaluation, are given for the case in which the elastic electron–ion-core scattering is described by the isotropic-scatterer model.

I. INTRODUCTION

In the first two papers of this series Duke and Laramore constructed a general, diagrammatic, quantum field theory of inelastic low-energy-electron diffraction[1] (ILEED) and used this theory to evaluate sample ILEED intensities in the simplest physically reasonable model[2]—that of "two-step" kinematical inelastic diffraction in which the incident electron loses energy in a forward-scattering event and is "turned around" by a single elastic backscattering from the lattice potential. In this model, two types of inelastic-scattering events occur: (elastic) diffraction before (energy) loss[3] (D-L) and loss before diffraction[4,5] (L-D). In the analysis of Laramore and Duke[2] both the elastic and loss processes were treated in first-order perturbation theory (by definition, the "kinematical" approximation). If multiple elastic scattering within individual layers of scatterers is considered this version of the theory of ILEED is analogous to the double-diffraction model of elastic low-energy-electron diffraction[6,7] (ELEED). The kinematical model of two-step inelastic diffraction has been applied to analyze ILEED intensities from Al(100),[2,7–9] W(100),[2,10] and Al(111).[8,9,11] In the latter case, the kinematical two-step analysis was used to extract from experimental ILEED intensities the dispersion relation of surface plasmons on nominally clean Al(111).[8,9,11]

This paper is devoted to the examination of the consequences of multiple-elastic-scattering events on the ILEED intensities predicted by the quantum field theory constructed by Duke and Laramore.[1] Stated in the language of their diagrammatic perturbation theory, the cross sections calculated herein are obtained by summation of *all* diagrams in which the incident electron has undergone a single loss event but an arbitrary number of elastic-scattering events both before and after that loss. This is an important issue because, both for the model used in this paper,[12] and for more general models,[13–17] these multiple-elastic-scattering processes are known to dominate the nature of the ELEED intensities. Therefore, one would expect them to be important in determining the ILEED intensities also. Indeed, probably our most significant conclusion drawn from the analysis presented in Papers III and IV of this series is that a judicious choice of the data to be analyzed permits the extraction from experimental ILEED intensities of surface-plasmon dispersion relations using the kinematical two-step model in spite of the documented importance of dynamical effects in inelastic as well as elastic electron-solid scattering.

We have divided our analysis into two parts. In this paper, we outline the derivation from the diagrammatic quantum field theory of the "dynamical" model expressions for the ILEED intensities. This task is accomplished in Sec. III following a review of the model Hamiltonian in Sec. II. Finally, in Sec. IV we present expressions for the cross sections, based on the isotropic-scatterer model of elastic electron–ion-core scattering, that are suitable for numerical evaluation. Many of the details of our derivations are relegated to appendices in order to render the body of the paper more readable. Sample numerical calculations for Al(100) and Al(111) are presented in the following paper (Paper IV in the series). A complete sum-

mary of our results and the conclusions drawn from them is given at the end of that concluding paper[18] in the series.

II. MODEL HAMILTONIAN

In deriving our expressions for the cross sections we utilize the microscopic quantum field theory of ILEED presented originally by Duke and Laramore[1] with the refinements and corrections introduced by Duke and Bagchi.[8,9]

The incident electron is considered to interact both with ion cores in a rigid lattice and with a continuous boson field which describes the plasmons. The effects of the incoherent inelastic collisions of the incident electrons with the individual valence electrons in the solid is simulated by propagator renormalization via an energy-independent electron-inelastic-collision mean free path.[6] We neglect finite-temperature effects,[19] although, if desired, the model easily could be extended to include them. Within this context, the model Hamiltonian on which we base our cross section calculations is specified by

$$\mathcal{H} = \mathcal{H}_{\mathrm{RL}} + U_{\mathrm{el}} + \mathcal{H}_l \ , \tag{1a}$$

$$\mathcal{H}_{\mathrm{RL}} = \sum_{\vec{k}} \frac{\hbar^2 k^2}{2m} c^{\dagger}_{\vec{k}} c_{\vec{k}} + \sum_{\vec{k},\vec{q},n} c^{\dagger}_{\vec{k}+\vec{q}}\, c_{\vec{k}} B(n;\ \vec{k}+\vec{q},\ \vec{k}) \ , \tag{1b}$$

$$B(n;\ \vec{k}+\vec{q},\ \vec{k}) = e^{-i\vec{q}\cdot\vec{R}_n}\, t_n(\vec{k}+\vec{q},\ \vec{k};\ \hbar^2k^2/2m) \ , \tag{1c}$$

$$U_{\mathrm{el}} = \sum_{\vec{q},\vec{k},n} c^{\dagger}_{\vec{k}+\vec{q}} c_{\vec{k}}\, T(n;\ \vec{k}+\vec{q},\ \vec{k}) \ , \tag{1d}$$

$$T(n;\ \vec{k}+\vec{q},\ \vec{k}) = e^{-i\vec{q}\cdot\vec{R}_n} h(n) \ , \tag{1e}$$

$$h(n) = \sum_{\vec{p}} e^{-i\vec{p}\cdot\vec{R}_n}\, t(\vec{p})\ (b^{\dagger}_{\vec{p}} + b_{-\vec{p}}) \ , \tag{1f}$$

$$\mathcal{H}_l = \sum_{\vec{p}} \hbar\omega(\vec{p})\ (b^{\dagger}_{\vec{p}} b_{\vec{p}} + \tfrac{1}{2}) \ . \tag{1g}$$

In Eqs. (1) $\mathcal{H}_{\mathrm{RL}}$ designates the rigid-lattice Hamiltonian, U_{el} the electron-loss-mode interaction, and $\mathcal{H}_l$ is the loss-mode Hamiltonian. The $c_{\vec{k}}$ are the electron annihilation operators; the $b_{\vec{p}}$ are those of the plasmons; the $t_n(\vec{k}', \vec{k}, E)$ are the individual elastic site-scattering amplitudes for the ion cores at sites located at $\vec{R}_n$ in the solid; the $t(\vec{p})$ are the electron-plasmon interaction vertices; and the $\hbar\omega(\vec{p})$ are the energies of these plasmons as a function of their quasimomenta $\vec{p}$. Polarization indices have been suppressed. We use the isotropic-scatterer version[12] of the electron–ion-core interaction in which the elastic scattering is described by an angle-independent-scattering amplitude

$$t_\lambda(\vec{k}', \vec{k}, E) = t_\lambda(E) = -\hbar^2\,(e^{2i\delta_\lambda(E)} - 1)/4\pi ikm \ , \tag{2}$$

in which $\delta_\lambda(E)$ is the s-wave phase shift for electrons of energy E scattered from the ion-core scatterers in a plane parallel to the surface labeled by λ. We usually presume all of the scatterers are electronically identical, i.e., $\delta_\lambda = \delta$ for all λ, although sometimes we permit the surface scatterers ($\delta_0 \equiv \delta_s$) to differ from those in the bulk ($\delta_\lambda = \delta_B$; $\lambda \neq 0$).

Our model for the loss-mode Hamiltonians U_{el} and $\mathcal{H}_l$ is that given by Bagchi and Duke.[9] In considering surface- and bulk-plasmon excitations, we can speak of the two loss processes as independent because the various normal modes of a metal obey an orthogonality condition,[20] thus permitting us to add their separate contributions to the scattering cross section.

The loss processes are specified by the loss-mode dispersion relations and their coupling vertices to the electrons. We display this information in the form of the loss-mode spectral density $\Lambda_\alpha(n, m, \omega)$ defined in Eq. (2.9) in Ref. 1. Here α designates the type of boson field, whereas m and n are indices labeling the scattering planes. For the case of surface plasmons the spectral density can be written as

$$\Lambda_s(n, m, \omega) = -\sum_{\vec{p}_\parallel} t^*_s(\vec{p}_\parallel)\, t_s(\vec{p}_\parallel)\, e^{-i\vec{p}_\parallel\cdot(\vec{R}_m - \vec{R}_n)} \times e^{-p_\parallel(|R_{m\perp}| + |R_{n\perp}|)} N(-\omega) 2i\, \mathrm{Im} D_s(\vec{p}_\parallel, \omega) \ , \tag{3}$$

in which $t_s(\vec{p}_\parallel)$ is the vertex function, $D_s(\vec{p}_\parallel, \omega)$ is the plasmon propagator, $\vec{R}_m$ and $\vec{R}_n$ are the location of scattering centers, and $N(\omega)$ is the Bose distribution function,

$$N(\omega) = (e^{\hbar\omega/\kappa T} - 1)^{-1} \ . \tag{4}$$

We use the vertex function[1,9]

$$t_s(\vec{p}_\parallel) = [(\pi e^2 \hbar\omega_s / p_\parallel)\Omega^2]^{1/2}\, \theta(p_{cs} - p_\parallel) \ . \tag{5}$$

Here Ω is the volume of a unit cell. The boson propagator is given by

$$D_s(\vec{p}_\parallel, \omega) = [\hbar\omega - \hbar\omega_s(p_\parallel) + i\Gamma_s(p_\parallel)]^{-1} - [\hbar\omega + \hbar\omega_s(p_\parallel) + i\Gamma_s(p_\parallel)]^{-1} \ , \tag{6}$$

where $\hbar\omega_s(p_\parallel)$ and $\Gamma_s(p_\parallel)$ are given by

$$\hbar\omega_s(p_\parallel) = \hbar\omega_s + C_1 p_\parallel + C_2 p_\parallel^2 \ , \tag{7}$$

$$\Gamma_s(p_\parallel) = \Gamma_s + D_1 p_\parallel + D_2 p_\parallel^2 \ . \tag{8}$$

For the excitation of bulk plasmons we use the coherent-coupling vertex in semi-infinite jellium as originally given by Gersten.[1,20,21] The loss-mode spectral density is

$$\Lambda_b(n, m, \omega) = -\sum_{\vec{p}} t^*_b(\vec{p}) t_b(\vec{p})\, e^{-i\vec{p}_\parallel\cdot(\vec{R}_m - \vec{R}_n)} \times 2\sin(p_\perp R_{m\perp}) \sin(p_\perp R_{n\perp}) N(-\omega) 2i\, \mathrm{Im} D_b(\vec{p}, \omega) , \tag{9}$$

where the solid is assumed to occupy all space for $z > 0$ and the vertex function is

$$t_b(\vec{p}) = -i\,[(\pi e^2 \hbar\omega_b / p^2)\Omega^2]^{1/2} \theta(p_{cb} - p) \ , \tag{10}$$

with p_{cb} denoting a cutoff in momentum.[22] The bulk-plasmon propagator is

$$D_b(\vec{p},\ \omega) = [\hbar\omega - \hbar\omega_b(p) + i\Gamma_b(p)]^{-1} - [\hbar\omega + \hbar\omega_b(p) + i\Gamma_b(p)]^{-1}, \quad (11)$$

and the plasmon dispersion relation is, to $O(p^2)$,

$$\hbar\omega_b(p) = \hbar\omega_b + Ap^2 \quad (12a)$$

while its damping is given by

$$\Gamma_b(p) = \Gamma_b + B_1 p^2 + B_2 p^4 . \quad (12b)$$

The electron-electron interaction term is not explicitly included in Eqs. (1) because we incorporate its consequences indirectly into the calculation via the propagator renormalization procedure postulated by Duke and Tucker[23] and subsequently derived by Duke and Laramore[1] (for bulk loss processes; surface losses are discussed by Feibelman *et al.*[20]). This procedure is defined by taking E and the momentum parallel to the surface, $\vec{k}_{\parallel}$, to be conserved, while using the poles of the single-electron propagator to define the (complex) component of its momentum, $k_{\perp}$, inside the solid.[1,23] We designate by $\vec{g}$ the reciprocal-lattice vectors of the (periodic) two-dimensional atomic layers parallel to the surface (out of which the solid is constructed[23,24]). We also let $\vec{k}$ and $\vec{k}'$ denote the electron momenta before and after scattering, their components parallel to the surface being given by $\vec{k}_{\parallel}$ and $\vec{k}'_{\parallel}$, respectively. In terms of these quantities we define the normal component of electron momentum inside the metal, associated with a beam characterized by $\vec{k}'_{\parallel} = \vec{k}_{\parallel} + \vec{g}$, via

$$k_{\perp}(\vec{g},\ E) = \{2m[E - \Sigma(E)]/\hbar^2 - (\vec{k}_{\parallel} + \vec{g})^2\}^{1/2}, \quad (13)$$

where $\Sigma(E)$ is the complex electronic self-energy inside the metal. The form of $\Sigma(E)$ that we use is that given by Duke *et al.*[6]:

$$\Sigma(E) = -V_0 - i\Gamma(E), \quad (14a)$$

$$\Gamma(E) = \frac{\hbar^2}{m\lambda_{ee}}\left(\frac{2m}{\hbar^2}(E + V_0)\right)^{1/2}, \quad (14b)$$

where V_0 is the inner potential and λ_{ee} is, by definition, twice the inelastic-collision mean free path of an electron. The normal component of electron momentum outside the metal, $\tilde{k}_{\perp}(\vec{g},\ E)$, is defined similarly to $k_{\perp}(\vec{g},\ E)$ in Eq. (13), but with $\Sigma(E)$ set equal to zero. As described by Duke and Bagchi,[8,9] both quantities are required in the description of surface-plasmon excitation.

III. VERTEX RENORMALIZATION

Within the framework of the above model Hamiltonian, the inelastic electron-solid scattering cross sections may be evaluated (in principle) to any desired accuracy by following the diagrammatic perturbation theory of Duke and Laramore.[1] In Paper II of this series,[2] Laramore and Duke performed this evaluation for the (simplest) case of a kinematical two-step inelastic diffraction mechanism in which contributions from the two lowest-order diagrams describing both elastic and energy-loss processes are added coherently in accordance with the quantum theory of scattering. Their calculation corresponds to evaluation of the diagrams shown in Figs. 1(a) and 1(b) for the case of diffraction before loss (D-L) and the loss before diffraction (L-D), respectively. Duke and Bagchi's calculation[8,9,11] is based on this same model, differing from that of Laramore and Duke only via the use of a more accurate treatment of electron interactions with surface plasmons.

The analysis presented in this paper extends the kinematic two-step model calculations by summation of all diagrammatic contributions to the cross section in which the electron has scattered elastically from the lattice an arbitrary number of times, but has undergone only a single loss event. It is convenient to divide these diagrams into three classes. First, we sum all of the diagrams in which one or more elastic-scattering events occur before the loss process. The sum of these diagrams defines a generalized D-L process, indicated diagrammatically in Fig. 1(c). Second, we sum all of the diagrams in which one or more elastic

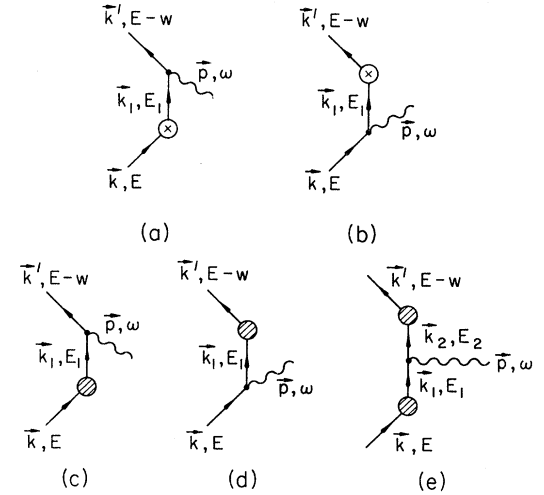

FIG. 1. Diagrams contributing to the scattering amplitudes of ILEED: (a) Two-step, diffraction before loss; (b) two-step, loss followed by diffraction; (c) multiple elastic diffraction before loss; (d) loss followed by multiple elastic diffraction; (e) multiple elastic diffraction both before and after loss. The perturbation-theory definition of the expressions for the cross sections associated with these diagrams is given by Duke and Laramore (Ref. 1). The shaded circle indicates the summation of an arbitrary number of individual elastic scattering events [designated by the circled cross in Figs. 1(a) and 1(b)].

scatterings occur after the loss event. This sum defines a generalized L-D process indicated diagrammatically in Fig. 1(d). Finally, we sum all of the diagrams in which the incident electron experiences one or more elastic scatterings *both* before and after the loss event. The sum of these diagrams defines a generalized diffraction-followed-by-loss-followed-by-diffraction (D-L-D) process indicated in Fig. 1(e).

The summations indicated in Figs. 1(c)–1(e) are elementary to carry out in practice because they yield simply an additional renormalization of the electron-layer vertices in the renormalized version of perturbation theory in which all electron–ion-core scattering events in a given layer have been summed.[2,6,23–25] Thus we proceed in two steps: First, we illustrate how this additional renormalization follows from the diagrammatic perturbation theory. Then, we show how to reduce the resulting formal expressions to forms suitable for the numerical evaluation of the cross sections. The nine diagrams describing the possible inelastic processes which include multiple elastic scattering from a rigid lattice and one loss step are shown in Fig. 2. The first four diagrams, Figs. 2(a)–2(d), correspond to the renormalized elastic D-L and the loss before the multiple diffraction processes. The remaining diagrams, Figs. 2(e)–2(i), describe the renormalized "three-step" process which involves multiple elastic diffractions both before and after the loss event. Specifically, Figs. 2(a) and 2(b) describe the processes of multiple elastic diffraction prior to loss and loss prior to elastic diffraction, respectively, whereas Figs. 2(c) and 2(d) represent the corresponding interference processes associated with the coherent nature of the two types of contributions to inelastic diffraction. Similarly, diagram 2(e) represents the physical "three-step" process while diagrams 2(f)–2(i) are associated with interference processes between renormalized three- and two-step processes.

In order to illustrate how the dynamical multiple-elastic-scattering vertex renormalization follows from the diagrammatic perturbation theory derived by Duke and Laramore[1] we examine the diagram in Fig. 2(a) (details of the renormalization of the "three-step" diagrams are given in Appendix A). In Fig. 3 we display diagrammatically this renormalization procedure. The elastic-scattering vertices in diagram 3(a), which are renormalized by multiple-elastic-diffraction processes from a rigid lattice, are obtained by summing an infinite number of diagrams containing a progressively increasing number of elastic-diffraction vertices as indicated in Figs. 3(b)–3(d). Diagram 3(b) is the two-step process considered in Paper II of this series,[2] which involves a single elastic diffraction process and single loss event, whereas Figs. 3(c), 3(d),

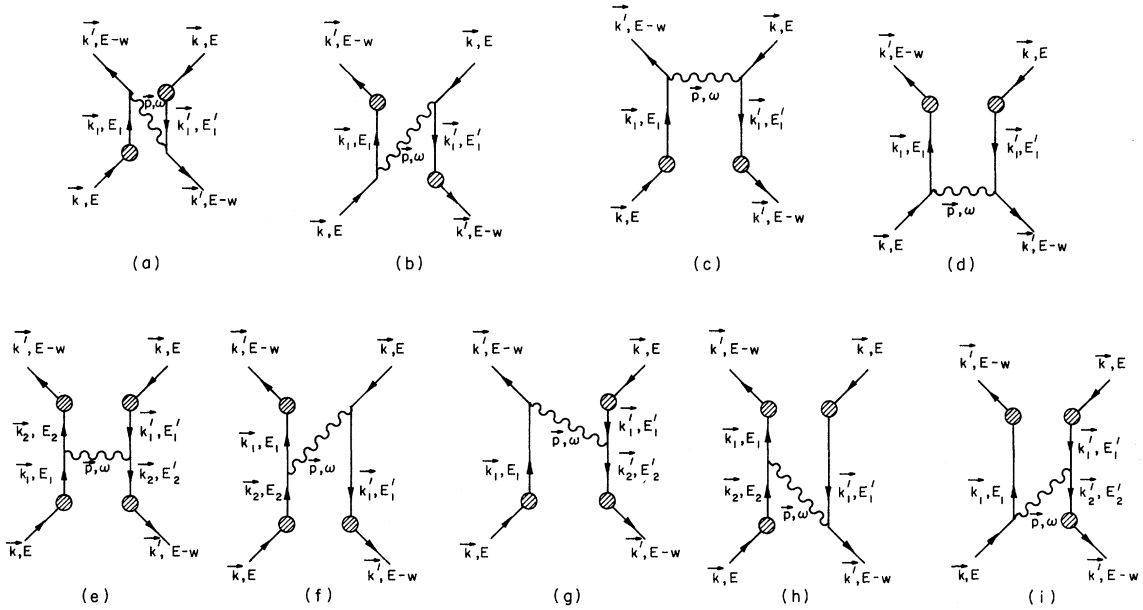

FIG. 2. Nine diagrams which contribute to the inelastic cross sections. (a) The physical process of diffraction prior to loss; (b) the process of loss prior to diffraction; (c) and (d) interference processes associated with the coherent nature of the contributions displayed in (a) and (b); (e) the process of diffraction before and after loss the event, the "three-step" process; (f)–(i) interference diagrams for the "three-step" process. The perturbation-theory definition of the expressions for the cross sections associated with these diagrams is given by Duke and Laramore (Ref. 1). The shaded circle indicates the summation of an arbitrary number of individual elastic-scattering events.

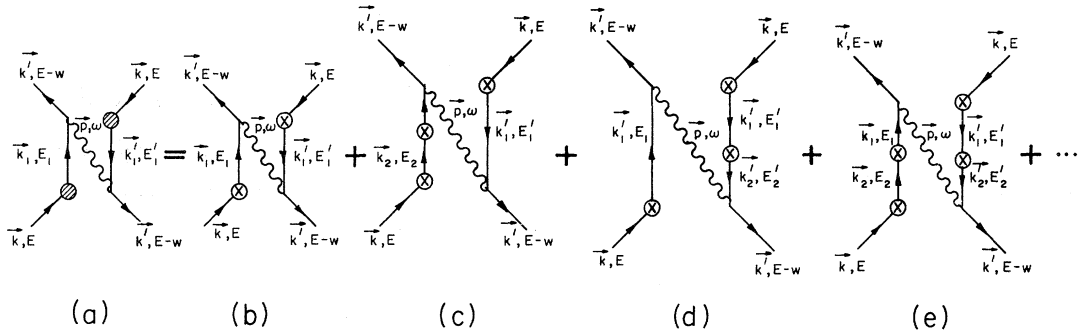

FIG. 3. A diagrammatic description of the renormalization procedure for the diffraction prior to loss process [e.g., Fig. 2(a)]. (a) The renormalized process of diffraction prior to loss; (b) two-step, diffraction before loss; (c)–(e) multiple-elastic-diffraction-before-loss diagrams, added up in the process of renormalization. The perturbation-theory definition of the expressions for the cross sections associated with these diagrams is given by Duke and Laramore (Ref. 1). The shaded circle indicates the summation of an arbitrary number of individual elastic-scattering events [designated by the circled cross in Figs. 1(a) and 1(b)].

etc., are the renormalizing diagrams composed of multiple-elastic-scattering processes and one loss. Following the diagrammatic prescription of Duke and Laramore[1] we obtain the following expressions for the contribution of a general term in the sum to the inelastic differential cross section:

$$\left(\frac{d^2\sigma}{d\Omega\,dE}\right)^{n+n'+1}=\left(\frac{m}{\hbar^2}\right)^2\left(\frac{E-w}{E}\right)^{1/2}[\delta(E-E'-\omega)]^{-1}\sum_{\vec{p},\vec{k}_1\vec{k}_1'}\int\frac{dw}{2\pi}(2\pi)^2\delta(E'-E_1+w)\delta(E-E_1'-w)$$
$$\times\sum_{n_0,n_0'}e^{-i(\vec{k}'-\vec{k}_1)\cdot\vec{R}_{n_0}}e^{-i(\vec{k}-\vec{k}_1')\cdot\vec{R}_{n_0'}}e^{-i\vec{p}\cdot(\vec{R}_{n_0}-\vec{R}_{n_0'})}t_{n_0}(\vec{p})t^*_{n_0'}(\vec{p})$$
$$\times\prod_{i=1}^{n}\int\frac{dE_i}{2\pi}\int\frac{d^3k_i}{(2\pi)^3}[2\pi\delta(E_i-E_{i+1})]G_R(\vec{k}_i,\,E_i)\sum_{n_i}e^{-i(\vec{k}_i-\vec{k}_{i+1})\cdot R_{n_i}}t_{n_i}(\vec{k}_i,\,\vec{k}_{i+1})$$
$$\times\prod_{j=1}^{n'}\int\frac{dE_j'}{2\pi}\int\frac{d^3k_j'}{(2\pi)^3}[2\pi\delta(E_j'-E_{j+1}')]G_A(\vec{k}_j',\,E_j')\sum_{n_j}e^{i(\vec{k}_j'-\vec{k}_{j+1}')\cdot\vec{R}_{n_j}}t_{n_j}(\vec{k}_j',\,\vec{k}_{j+1}').\qquad(15)$$

In Eq. (15) G_R is the retarded electron propagator given by

$$G^{-1}(\vec{k},\,E)=E-\frac{\hbar^2k^2}{2m}-\Sigma(\vec{k},\,E)\qquad(16)$$

with the self-energy $\Sigma(\vec{k},\,E)$ defined by Eq. (14a) for our numerical calculations discussed in Sec. III. G^A is the advanced electron propagator defined by $G_A=G_R^*$. We use the notation $E_{n+1}=E$, $\vec{k}_{n+1}=\vec{k}$, and $E_{n'+1}=E'$, $\vec{k}_{n'+1}=\vec{k}'$, and $n,\,n'\geq 1$.

In order to calculate the full contribution from the diagram in Fig. 3(a) we must sum over all n and n' in Eq. (15). Assuming that all scattering sites in a given subplane parallel to the surface are equivalent[24] (i.e., we take the potential at a given site to depend only on the distance of that site from the surface), the total contribution from Diagram 3(a) can be expressed in a more convenient way by defining the scattering amplitude $R(\vec{k}',\,\vec{k};\,E)$,[24,25]

$$R(\vec{k}',\,\vec{k};\,E)=\frac{(2\pi)^2}{A}\sum_{\lambda}\sum_{\vec{g}}e^{-i(k_\perp'-k_\perp)d\lambda-i\vec{g}\cdot\vec{a}\lambda}$$
$$\times T_\lambda(\vec{k}',\,\vec{k};\,E)\delta(\vec{k}_{\parallel}'-\vec{k}_{\parallel}-\vec{g}),\qquad(17a)$$
$$T_\lambda(\vec{k}',\,\vec{k};\,E)=\tau_\lambda(\vec{k}',\,\vec{k};\,E)+\sum_{\vec{k}_1}\sum_{\lambda_1\neq\lambda}\tau_\lambda(\vec{k}',\,\vec{k}_1;\,E)$$
$$\times G^{\lambda\lambda_1}(\vec{k}_1,\,\vec{k};\,E)T_{\lambda_1}(\vec{k}_1,\,\vec{k};\,E),\qquad(17b)$$
$$\tau_\lambda(\vec{k}',\,\vec{k};\,E)=t_\lambda(\vec{k}',\,\vec{k};\,E)+\sum_{\vec{k}_1}t_\lambda(\vec{k}',\,\vec{k}_1;\,E)$$
$$\times G^{sp}(\vec{k}_1,\,\vec{k};\,E)\tau_\lambda(\vec{k}_1,\,\vec{k};\,E),\qquad(17c)$$
$$G^{\lambda\lambda_1}(\vec{k}_1,\,\vec{k};E)=\sum_{\vec{P}}\exp\{-i(\vec{k}_{1\parallel}-\vec{k}_{\parallel})\cdot[\vec{P}+\vec{a}(\lambda_1-\lambda)]$$
$$-i(k_{1\perp}-k_\perp)(d\lambda_1-d\lambda)\}G(\vec{k}_1,E),\qquad(17d)$$
$$G^{sp}(\vec{k}_1,\vec{k};E)=\sum_{\vec{P}\neq 0}e^{-i(\vec{k}_{1\parallel}-\vec{k}_{\parallel})\cdot\vec{P}}G(\vec{k}_1;E).\qquad(17e)$$

The vector $\vec{P}$ designates points in the Bravais net of the individual (identical) subplanes, A is the

area of a primitive unit cell of the subplane, $\lambda\vec{a}$ is the position of the origin in the λth subplane, and $d\lambda$ is the distance of the λth subplane below the surface which is taken to be the plane $z=0$. Equations (17) completely define the renormalized elastic-cross section vertex. We also define the crystal loss amplitude as

$$T(\vec{k}', \vec{k}, \vec{p}) = \frac{2\pi m}{h^2} \sum_n e^{-i(\vec{k}'-\vec{k}-\vec{p})\cdot\vec{R}_n} t_n(\vec{p}) \ . \qquad (18)$$

The central point illustrated by Fig. 3 is conceptually simple although algebraically complicated. As we write the sum of all the contributions of the form given by Eq. (15) associated with the diagrams shown in Figs. 3(b)–3(e), we generate a series in which the square of the inelastic vertex, Eq. (18), is a common factor. This sum can be rewritten as an amplitude squared. This amplitude is itself a sum over elastic-scattering events multipled by an inelastic-scattering vertex. By inspection of the sum over elastic events in this amplitude, we see that this sum specifies the total elastic-scattering amplitude $R(\vec{k}', \vec{k}, E)$ defined by Duke and coworkers[19,25] and given by Eqs. (17). Thus we establish that in the theory of the inelastic as well as the theory of elastic LEED the summation of multiple-elastic-scattering events leads to the dynamic elastic-scattering amplitude $R(\vec{k}', \vec{k}, E)$ defined by Eqs. (17), rather than the kinematical elastic-scattering amplitude [defined by $T_\lambda \to t_\lambda$ in Eq. (17a)].

In terms of the dynamical elastic-scattering amplitude given by Eqs. (17) and the kinematical inelastic amplitude given by Eq. (18), the contribution to the inelastic-scattering cross sections associated with Fig. 3(a) is given by

$$\left(\frac{d^2\sigma}{d\Omega\, dE}\right)^{\text{D-L}} = \left(\frac{E-w}{E}\right)^{1/2}\left(\frac{-iN(-w)}{\pi}\right)\sum_{\vec{p}} \text{Im}D(\vec{p}, w) \times \left| A_1'(\vec{k}', \vec{k}, \vec{p}, E, w)\right|^2 \ , \qquad (19)$$

in which

$$A_1'(\vec{k}', \vec{k}, \vec{p}, E, w) = \int \frac{d^3k_1}{(2\pi)^3}\, T(\vec{k}', \vec{k}_1, \vec{p})\, G^R(\vec{k}_1, E) \times R(\vec{k}_1, \vec{k}, E) \qquad (20)$$

is the scattering amplitude for the whole inelastic process [see, e.g., Fig. (1c)]. Similarly, the amplitude for the renormalized L-D process [Fig. 2(b) or 1(d)] is given by

$$A_2'(\vec{k}', \vec{k}, \vec{p}, E, w) = \int \frac{d^3k_1}{(2\pi)^3}\, R(\vec{k}', \vec{k}_1, E-w) \times G^R(\vec{k}_1, E-w)\, T(\vec{k}_1, \vec{k}, \vec{p}) \ . \qquad (21)$$

Finally, the amplitude for the "three-step" process [see Fig. 2(e) or 1(e)] is specified by

$$A_3'(\vec{k}', \vec{k}, \vec{p}, E, w) = \int \frac{d^3k_1}{(2\pi)^3} \int \frac{d^3k_2}{(2\pi)^3}\, R(\vec{k}', \vec{k}_1, E-w) \times G(\vec{k}_1, E-w)\, T(\vec{k}_1, \vec{k}_2, \vec{p}) \times G^R(\vec{k}_2, E) R(\vec{k}_2, \vec{k}, E) \ . \qquad (22)$$

In concluding this section we reemphasize that the two effects of multiple elastic diffraction are the replacement of the t_λ by T_λ [defined in Eqs. (17b)–(17e)] in the D-L and L-D contributions to the cross section [i.e., Figs. 1(b) and 1(c)], and the introduction of the D-L-D contribution to the cross section as illustrated in Fig. 1(d). The remainder of this paper is devoted to reducing the general formulas (19)–(22) to a form suitable for numerical computation. The following paper[18] contains our discussion of the consequences of these final formulas.

IV. FINAL EXPRESSIONS FOR THE CROSS SECTION

Following the method of analysis outlined in Sec. III and Appendix A, we obtain the expression for the inelastic-scattering differential cross section which includes the contributions from all nine diagrams in Fig. 2:

$$\left(\frac{d^2\sigma}{d\Omega\, dE}\right) = \left(\frac{E-w}{E}\right)^{1/2} \sum_{\vec{p}} \left(\frac{-iN(-w)}{\pi}\, \text{Im}D(\vec{p}, w)\right) \times \left| \sum_{i=1}^{3} A_i'(\vec{k}', \vec{k}, \vec{p}, E, w)\right|^2 \ . \qquad (23)$$

By taking the square modulus of the coherent sum of the three scattering amplitudes [Eqs. (20)–(22)] we include contributions from the interference diagrams as well as the direct ones. Using the two-dimensional periodicity in the layers we performed the summations indicated in the above formulas to derive the final expressions for the surface and bulk contributions to the differential inelastic-scattering cross section. (The details of a sample calculation are displayed in Appendix B.) For the sake of clarity in the presentation we introduce the following quantities:

$$R[k_\perp, \vec{g}, u; k_\perp', \vec{g}', w; p, \vec{g}''] \equiv \exp(i\{[k_\perp(\vec{g}, E-u) + k_\perp'(\vec{g}', E-w)]d - \vec{g}''\cdot\vec{a}\} - pd) \ , \qquad (24)$$

$$R_a^\lambda[k_\perp, \vec{g}, u; k_\perp', \vec{g}', w; p, \vec{g}''] \equiv 1 - R^\lambda[k_\perp, \vec{g}, u; k_\perp', \vec{g}', w; p, \vec{g}''] \ , \qquad (25)$$

$$TR^{\lambda,\lambda_1}[v; k_\perp, \vec{g}, u; k_\perp', \vec{g}', w; p, \vec{g}''] \equiv \sum_{\lambda=\lambda_1}^{\infty} T_\lambda(E-v) R^\lambda[k_\perp, \vec{g}, u; k_\perp', \vec{g}', w, p, \vec{g}''] \ . \qquad (26)$$

The quantity $k_\parallel'$, the parallel momentum of the

exiting electron, is given in terms of the exit-beam parameters w, the loss energy, and θ', the polar exit angle, via

$$k'_{\parallel}=\left(\frac{2m}{\hbar^2}(E-w)\right)^{1/2}\sin\theta' \ . \tag{27}$$

Using these quantities, the various contributions to the cross section can be written in the fashion indicated below.

A. Surface Contribution

The surface contribution to the differential cross section for the inelastic scattering of electrons by the surface-plasmon field is given by

$$\left(\frac{d^2\sigma}{dE\,d\Omega}\right)_{sp}=\left(\frac{E-w}{E}\right)^{1/2}\frac{2\pi m}{h^2}\,\frac{m\pi e^2\hbar\omega_s}{h^2}\,\frac{\Omega^2}{A}\sum_{\vec{g}\vec{g}_1\vec{g}_2}\sum_{(\vec{g}_1+\vec{g}_2=\vec{g})}\frac{2\Gamma_s(\vec{p}_{\parallel})}{[w-\hbar\omega_s(\vec{p}_{\parallel})]^2+[\Gamma_s(\vec{p}_{\parallel})]^2}$$

$$\times\frac{1}{[p_{\parallel}^2+(\Gamma_s/c_1)^2]^{1/2}}\left|A_1(\vec{k}',\vec{k},\vec{p},E,w)+A_2(\vec{k}',\vec{k},\vec{p},E,w)+A_3(\vec{k}',\vec{k},\vec{p},E,w)\right|^2 . \tag{28}$$

In this equation, the plasmon momentum is given by

$$\vec{p}_{\parallel}=\vec{k}'_{\parallel}-\vec{k}_{\parallel}-\vec{g} \ ; \tag{29}$$

Ω and A are the volume and area of a unit cell and $\vec{g}$ is the external exiting-beam index (note the restriction on the beams exiting from the "three-step" processes, $\vec{g}_1+\vec{g}_2=\vec{g}$). In calculating the surface contribution to the cross section we have included the interaction of the incoming electron with the surface-plasmon field outside as well as inside the metal.[8]

The three contributions, A_i, to the diffraction amplitude are best considered separately.

(i) Diffraction before loss (D-L):

$$A_1(\vec{k}',\vec{k},\vec{p},E,w)=-\frac{im}{\hbar^2Ak_{\perp}(\vec{g},E)}\left(\frac{TR^{\lambda,0}[0;k_{\perp},0,0;k_{\perp},\vec{g},0;0,\vec{g}]}{i[\vec{k}'_{\perp}(0,E-w)-\vec{k}_{\perp}(\vec{g},E)]d+p_{\parallel}d}\right.$$

$$\left.+\sum_{\lambda=0}^{\infty}T_{\lambda}(E)R^{\lambda}[k_{\perp},0,0;k_{\perp},\vec{g},0;0,\vec{g}]\frac{R_a^{\lambda+1}[k'_{\perp},0,w;-k_{\perp},\vec{g},0;p_{\parallel},0]}{R_a[k'_{\perp},0,w;-k_{\perp},\vec{g},0;p_{\parallel},0]}\right) . \tag{30}$$

(ii) Loss before diffraction (L-D):

$$A_2(\vec{k}',\vec{k},\vec{p},E,w)=-\frac{im}{\hbar^2Ak_{\perp}(-\vec{g},E-w)}\,\frac{TR^{\lambda,0}[w;k'_{\perp},-\vec{g},w;k'_{\perp},0,w;0,\vec{g}]}{i[\vec{k}_{\perp}(0,E)-\vec{k}_{\perp}(-\vec{g},E-w)]d+p_{\parallel}d}$$

$$\times\sum_{\lambda=0}^{\infty}T_{\lambda}(E-w)R^{\lambda}[k'_{\perp},-\vec{g},w;k'_{\perp},0,w;0,\vec{g}]\,\frac{R_a^{\lambda+1}[k_{\perp},0,0;-k'_{\perp},-\vec{g},w;p_{\parallel},0]}{R_a[k_{\perp},0,0;-k'_{\perp},-\vec{g},w;p_{\parallel},0]} \ . \tag{31}$$

(iii) Diffraction before and after loss (D-L-D): For the "three-step" process we distinguish between two sets of layer sums. Let us denote the layers at which a loss occurs by the layer index λ_3. The layers at which multiple-elastic-diffraction processes take place before and after the loss step are assigned the indices λ_1 and λ_2, respectively. Using this designation of indices, the two sets of summations indicated above are

$$S_3^a \text{ when } \lambda_1<\lambda_3<\lambda_2 \ , \tag{32a}$$

$$S_3^b \text{ when } \lambda_1>\lambda_3>\lambda_2 \ . \tag{32b}$$

Due to the forward scattering nature of the plasmon-emission vertices, the above two sets are the only ones that have to be considered and $\lambda_3>0$ always, so that the coupling to surface plasmons outside the solid does not contribute to the "three-step" diagrams. The expression for the D-L-D amplitude is given by

$$A_3(\vec{k}',\vec{k},\vec{p},E,w)=-\frac{im}{\hbar^2Ak_{\perp}(\vec{g}_1,E)}\,\frac{-im}{\hbar^2Ak'_{\perp}(-\vec{g}_2,E-w)}$$

$$\times[S_3^a(\vec{g}_1,\vec{g}_2,\vec{k},E,w,p_{\parallel})$$

$$+S_3^b(\vec{g}_1,\vec{g}_2,\vec{k},E,w,p_{\parallel})] \ , \tag{33}$$

$$S_3^a=\{R_a[k_{\perp},\vec{g}_1,0;-k'_{\perp}-\vec{g}_2,w;p_{\parallel},0]\}^{-1}[A-B] \ ,$$

$$A=TR^{\lambda_1,0}[0;k_{\perp},0,0;-k'_{\perp},-\vec{g}_2,w;p_{\parallel},\vec{g}_1]$$

$$\times TR^{\lambda_2,\lambda_1}[\omega;k'_{\perp},-\vec{g}_2,w;k'_{\perp},0,w;0,\vec{g}_2] \ , \tag{34}$$

$$B=R[k_{\perp},\vec{g}_1,0;-k'_{\perp},-\vec{g}_2,w;p_{\parallel},0]$$

$$\times TR^{\lambda_1,0}[0;k_{\perp},0,0;-k_{\perp},\vec{g}_1,0;0,\vec{g}_1]$$

$$\times TR^{\lambda_2,\lambda_1}[w;k_{\perp},\vec{g}_1,0;k'_{\perp},0,w;p_{\parallel},\vec{g}_2] \ ,$$

$$S_3^b = \{R_a[k_\perp', -\vec{g}_2, w; -k_\perp, \vec{g}_1, 0; p_\parallel, 0]\}^{-1}[C - D],$$

$$C = TR^{\lambda_2,0}[\omega; k_\perp', 0, \omega; -k_\perp, \vec{g}_1, 0; p_\parallel, \vec{g}_2] \times TR^{\lambda_1,\lambda_2}[0; k_\perp, 0, 0; k_\perp, \vec{g}_1, 0; 0, \vec{g}_1], \quad (35)$$

$$D = R[k_\perp', -\vec{g}_2, w; -k_\perp, \vec{g}_1, 0; p_\parallel, 0] \times TR^{\lambda_2,0}[w; k_\perp', 0, w; -k_\perp', -\vec{g}_2, w; 0, \vec{g}_2] \times TR^{\lambda_1,\lambda_2}[0; k_\perp, 0, 0; k_\perp', -\vec{g}_2, w; p_\parallel, \vec{g}_1].$$

B. Bulk Contributions

The expression for the contributions to the differential cross section by the inelastic processes that the scattered electron undergoes in the bulk is given by

$$\left(\frac{d^2\sigma}{dE\,d\Omega}\right)_{bp} = \left(\frac{E-w}{E}\right)^{1/2} \frac{2\pi m}{h^2} \frac{m\pi e^2\hbar\omega_b}{h^2} \frac{\Omega^2}{2A} \int_0^{p_{cb}} \frac{dp_\perp}{\pi} \frac{1}{p_\parallel^2 + p_\perp^2 + (\Gamma_b(\vec{p}_\parallel, p_\perp)/A)} \times \frac{2\Gamma_b(\vec{p}_\parallel, p_\perp)}{[w - \hbar\omega_b(\vec{p}_\parallel, p_\perp)]^2 + \Gamma_b^2(\vec{p}_\parallel, p_\perp)} \left|A_1(\vec{k}', \vec{k}, \vec{p}, E, w) + A_2(\vec{k}', \vec{k}, \vec{p}, E, w) + A_3(\vec{k}', \vec{k}, \vec{p}, E, w)\right|^2. \quad (36)$$

As before, we specify the three contributions to the diffraction amplitude separately.

(i) Diffraction before loss (D-L):

$$A_1(\vec{k}', \vec{k}, \vec{p}, E, w) = -\frac{m}{\hbar^2 A k_\perp(\vec{g}, E)} \sum_{\lambda=0} T_\lambda(E) R^\lambda[k_\perp, 0, 0; k_\perp, \vec{g}, 0; 0, \vec{g}] \times \left(\frac{R_a^{\lambda+1}[k_\perp', 0, w; -k_\perp, \vec{g}, 0; -ip_\perp, 0]}{R_a[k_\perp', 0, w; -k_\perp, \vec{g}, 0; -ip_\perp, 0]} - \frac{R_a^{\lambda+1}[k_\perp', 0, w; -k_\perp, \vec{g}, 0; ip_\perp, 0]}{R_a[k_\perp', 0, w; -k_\perp, \vec{g}, 0; ip_\perp, 0]}\right). \quad (37)$$

(ii) Loss before diffraction (L-D):

$$A_2(\vec{k}', \vec{k}, \vec{p}, E, w) = -\frac{m}{\hbar^2 A k_\perp'(-\vec{g}, E-w)} \sum_{\lambda=0}^{\infty} T_\lambda(E-w) R^\lambda[k_\perp', 0, w; k_\perp', -\vec{g}, \omega; 0, \vec{g}] \times \left(\frac{R_a^{\lambda+1}[k_\perp, 0, 0; -k_\perp', -\vec{g}, w; -ip_\perp, 0]}{R_a[k_\perp, 0, 0; -k_\perp', -\vec{g}, w; -ip_\perp, 0]} - \frac{R_a^{\lambda+1}[k_\perp, 0, 0; -k_\perp', -\vec{g}, w; ip_\perp, 0]}{R_a[k_\perp, 0, 0; -k_\perp', -\vec{g}, w; ip_\perp, 0]}\right). \quad (38)$$

(iii) Diffraction before and after loss (D-L-D):

$$A_3(\vec{k}', \vec{k}, \vec{p}, E, w) = -\frac{m}{\hbar^2 A k_\perp(-\vec{g}_2, E-w)} \frac{-im}{\hbar^2 A k_\perp(\vec{g}_1, E)} [S_3^a(\vec{g}_1, \vec{g}_2, \vec{k}, E, w, \pm ip_\perp) + S_3^b(\vec{g}_1, \vec{g}_2, \vec{k}, E, w, \pm ip_\perp)], \quad (39)$$

$$S_3^a = \sum_{\lambda_1=0}^{\infty} T_{\lambda_1}(E) \sum_{\lambda_2=\lambda_1}^{\infty} T_{\lambda_2}(E-w) R^{\lambda_1}[k_\perp, 0, 0; -k_\perp, \vec{g}_1, 0; 0, \vec{g}_1] R^{\lambda_2}[k_\perp', 0, w; k_\perp', -\vec{g}_2, w; 0, \vec{g}_2]$$

$$\times \left(\frac{R^{\lambda_1}[k_\perp, \vec{g}_1, 0; -k_\perp', -\vec{g}_2, w; -ip_\perp, 0] - R^{\lambda_2+1}[k_\perp, \vec{g}_1, 0; -k_\perp', -\vec{g}_2, w; -ip_\perp, 0]}{R_a[k_\perp, \vec{g}_1, 0; -k_\perp', -\vec{g}_2, w; -ip_\perp, 0]} - \frac{R^{\lambda_1}[k_\perp, \vec{g}_1, 0; -k_\perp', \vec{g}_2, w; ip_\perp, 0] - R^{\lambda_2+1}[k_\perp', \vec{g}_1, 0; -k_\perp, -\vec{g}_2, w; ip_\perp, 0]}{R_a[k_\perp, \vec{g}_1, 0; -k_\perp', -\vec{g}_2, w; ip_\perp, 0]}\right), \quad (40)$$

$$S_3^b = \sum_{\lambda_2=0}^{\infty} T_{\lambda_2}(E-w) \sum_{\lambda_1=\lambda_2}^{\infty} T_{\lambda_1}(E) R^{\lambda_2}[k_\perp', 0, w; -k_\perp', -\vec{g}_2, w; 0, \vec{g}_2] R^{\lambda_1}[k_\perp, 0, 0; k_\perp, \vec{g}_1, 0; 0, \vec{g}_1]$$

$$\times \left(\frac{R^{\lambda_2}[k_\perp', -\vec{g}_2, w; -k_\perp, \vec{g}_1, 0; -ip_\perp, 0] - R^{\lambda_1+1}[k_\perp', -\vec{g}_2, w; -k_\perp, \vec{g}_1, 0; -ip_\perp, 0]}{R_a[k_\perp', -\vec{g}_2, w; -k_\perp, \vec{g}_1, 0; -ip_\perp, 0]} - \frac{R^{\lambda_2}[k_\perp', -\vec{g}_2, w; -k_\perp, \vec{g}_1, 0; ip_\perp, 0] - R^{\lambda_1+1}[k_\perp', -\vec{g}_2, w; -k_\perp, \vec{g}_1, 0; ip_\perp, 0]}{R_a[k_\perp', -\vec{g}_2, w; -k_\perp, \vec{g}_1, 0; ip_\perp, 0]}\right). \quad (41)$$

Equations (23)–(41) are the expressions used in all of the numerical calculations described in the following paper.[18] In the kinematical limit, $T_\lambda \to t_\lambda = t$, they reduce to the formulas derived by Duke and

Bagchi.[8,9] In the general "dynamical" case, a discussion of their consequences is given in the following paper.

APPENDIX A

This Appendix is devoted to the description of the renormalization, due to the summation of multiple-elastic-scattering events, of the amplitudes of the inelastic processes. The expressions for the cross sections and amplitudes of the inelastic diffraction of low-energy electrons scattered from a solid are given in the text by Eqs. (23) and (20)–(22), respectively. In order to demonstrate the renormalization procedure, we discuss the amplitude of the "three-step" process since the generalized "two-step" processes of diffraction prior to loss and vice versa follow easily from it as special cases. The renormalization of the elastic vertices indicated in Fig. 4(a) is performed in the following steps.

(1) The contribution to the amplitude from processes involving multiple-elastic-scattering events before the loss process and *only one* elastic-scattering event after the loss step is summed first, as illustrated by the summation of diagrams 4(b1), 4(c1), etc.

(2) The contribution to the amplitude from processes involving multiple-elastic-scattering events before the loss process and *two* elastic scattering events after the loss step is summed and added to the amplitude resulting from the renormalization step 1. This is illustrated in Figs. 4(b2), 4(c2), etc.

The total renormalization is achieved by following the above steps with a sequentially increasing number of elastic-scattering events after the loss process, as is depicted in Figs. 4(b3), 4(c3), etc. By summing the contributions described above, we renormalize both the elastic diffraction prior to loss and the loss followed by elastic diffraction processes.

Following the diagrammatic rules of Duke and Laramore[1] we can write the algebraic realization of step (1) in the renormalization procedure. The amplitude corresponding to Fig. 4(b1) is given by

$$A'_{b1}(\vec{k}',\vec{k},\vec{p},E,w)=\frac{2\pi m}{h^2}\sum_{n_0}\sum_{n_1 n_{\bar{1}}}\int\frac{d^3k_1}{(2\pi)^3}\int\frac{d^3k_{\bar{1}}}{(2\pi)^3}\,e^{-i(\vec{k}_{\bar{1}}-\vec{k}_1-\vec{p})\cdot\vec{R}_{n_0}}\,t_{n_0}(\vec{p})\,e^{-i(\vec{k}_1-\vec{k})\cdot\vec{R}_{n_1}}\,G^R(\vec{k}_1,E)\,t_{n_1}(\vec{k}_1,\vec{k},E)$$
$$\times\,e^{-i(\vec{k}'-\vec{k}_{\bar{1}})\cdot\vec{R}_{n_{\bar{1}}}}\,G^R(\vec{k}_{\bar{1}},E-w)\,t_{n_{\bar{1}}}(\vec{k}',\vec{k}_{\bar{1}},E-w)\,. \tag{A1}$$

Similarly the contribution of Fig. 4(c1) is given by

$$A'_{c1}(\vec{k}',\vec{k},\vec{p},E,w)=\frac{2\pi m}{h^2}\sum_{n_0}\sum_{\substack{n_1,n_2,n_{\bar{1}}\\ n_1\neq n_2}}\int\frac{d^3k_1}{(2\pi)^3}\int\frac{d^3k_2}{(2\pi)^3}\int\frac{d^3k_{\bar{1}}}{(2\pi)^3}\,e^{-i(\vec{k}_{\bar{1}}-\vec{k}_1-\vec{p})\cdot\vec{R}_{n_0}}\,t_{n_0}(\vec{p})\,e^{-i(\vec{k}_2-\vec{k})\cdot\vec{R}_{n_2}}\,G^R(\vec{k}_2,E)\,t_{n_2}(\vec{k}_2,\vec{k},E)$$
$$\times\,e^{-i(\vec{k}_1-\vec{k}_2)\cdot\vec{R}_{n_1}}\,G^R(\vec{k}_1,E)\,t_{n_1}(\vec{k}_1,\vec{k}_2,E)\,e^{-i(\vec{k}'-\vec{k}_{\bar{1}})\cdot\vec{R}_{n_{\bar{1}}}}\,G^R(k_{\bar{1}},E-w)\,t_{n_{\bar{1}}}(\vec{k}',\vec{k}_{\bar{1}},E-w)\,. \tag{A2}$$

Summing the diagrams in step (1) we get

$$A_1^T=\sum_{S=b,c,\ldots}A'_{S1}=\frac{2\pi m}{h^2}\sum_{n_0}\int\frac{d^3k_1}{(2\pi)^3}\int\frac{d^3k_{\bar{1}}}{(2\pi)^3}\,e^{-i(\vec{k}_{\bar{1}}-\vec{k}_1-\vec{p})\cdot\vec{R}_{n_0}}\,t_{n_0}(\vec{p})\,G^R(\vec{k}_1,E)\,G^R(\vec{k}_{\bar{1}},E-w)$$
$$\times\Big[\sum_{n_{\bar{1}}}e^{-i(\vec{k}'-\vec{k}_{\bar{1}})\cdot\vec{R}_{n_{\bar{1}}}}\,t_{n_{\bar{1}}}(\vec{k}',\vec{k}_{\bar{1}},E-w)\Big]\Big\{\sum_{n_1}e^{-i(\vec{k}_1-\vec{k})\cdot\vec{R}_{n_1}}\,t_{n_1}(\vec{k}_1,\vec{k},E)+\sum_{n_1}\int\frac{d^3k_2}{(2\pi)^3}\,e^{-i(\vec{k}_1-\vec{k}_2)\cdot\vec{R}_{n_1}}$$
$$\times t_{n_1}(\vec{k}_1,\vec{k}_2,E)\,G^R(\vec{k}_2,E)\sum_{n_2\neq n_1}e^{-i(\vec{k}_2-\vec{k})\cdot\vec{R}_{n_2}}\,t_{n_2}(\vec{k}_2,\vec{k},E)+\cdots\Big\}\,. \tag{A3}$$

The expression in curly brackets on the right-hand side of Eq. (A3) is the scattering amplitude for the elastic processes occurring prior to the loss event, i.e., $T(\vec{k}_1,\vec{k},E)$.

Following the same procedure we get for the contribution of the diagrams in step (2):

$$A_2^T=\sum_{S=b,c,\ldots}A'_{S2}=\frac{2\pi m}{h^2}\sum_{n_0}\int\frac{d^3k_1}{(2\pi)^3}\int\frac{d^3k_{\bar{1}}}{(2\pi)^3}\,e^{-i(\vec{k}_{\bar{1}}-\vec{k}_1-\vec{p})\cdot\vec{R}_{n_0}}\,t_{n_0}(\vec{p})\,G^R(\vec{k}_1,E)\,G^R(\vec{k}_{\bar{1}},E-w)$$

$$\times\left(\sum_{n_{\bar{1}}}\sum_{n_{\bar{2}}\neq n_{\bar{1}}}\int\frac{d^3k_{\bar{2}}}{(2\pi)^3}e^{-i(\vec{k}_{\bar{2}}-\vec{k}_{\bar{1}})\cdot\vec{R}_{n_{\bar{1}}}}\,t_{n_{\bar{1}}}(\vec{k}_{\bar{2}},\vec{k}_{\bar{1}},E-w)\,G^R(\vec{k}_{\bar{2}},E-w)\,e^{-i(\vec{k}'-\vec{k}_{\bar{2}})\cdot\vec{R}_{n_{\bar{2}}}}\,t_{n_{\bar{2}}}(\vec{k}',\vec{k}_{\bar{2}},E-w)\right)T(\vec{k}_1,\vec{k},E)\,. \tag{A4}$$

The total renormalization is achieved by summing the A_m^T's over all m, yielding:

$$A_3'(\vec{k}',\vec{k},\vec{p},E,w)=\sum_{m=1}A_m^T=\frac{2\pi m}{\hbar^2}\int\frac{d^3k_1}{(2\pi)^3}\int\frac{d^3k_{\bar{1}}}{(2\pi)^3}\,T(\vec{k}_{\bar{1}},\vec{k}_1,\vec{p})\,G^R(\vec{k}_1,E)\,G^R(\vec{k}_{\bar{1}},E-w)\,T(\vec{k}',\vec{k}_{\bar{1}},E-w)\,T(\vec{k}_1,\vec{k},E)\,, \tag{A5}$$

where the scattering amplitude for the elastic processes occurring after the loss is given by

$$T(\vec{k}',\vec{k}_{\bar{1}},E-w)\equiv\sum_{n_{\bar{1}}}e^{-i(\vec{k}'-\vec{k}_{\bar{1}})\cdot\vec{R}_{n_{\bar{1}}}}\,t_{n_1}(\vec{k}',\vec{k}_{\bar{1}},E-w)+\sum_{n_{\bar{1}}}\int\frac{d^3k_{\bar{2}}}{(2\pi)^3}e^{-i(\vec{k}_{\bar{2}}-\vec{k}_{\bar{1}})\cdot\vec{R}_{n_{\bar{1}}}}\,t_{n_{\bar{1}}}(\vec{k}_{\bar{2}},\vec{k}_{\bar{1}},E-w)$$
$$\times G^R(\vec{k}_{\bar{2}},E-w)\sum_{n_{\bar{2}}\neq n_{\bar{1}}}e^{-i(\vec{k}'-\vec{k}_{\bar{2}})\cdot\vec{R}_{n_{\bar{2}}}}\,t_{n_{\bar{2}}}(\vec{k}',\vec{k}_{\bar{2}},E-w)+\cdots \tag{A6}$$

and the crystal-loss amplitude is given by

$$T(\vec{k}_{\bar{1}},\vec{k}_1,\vec{p})\equiv\sum_{n_0}e^{-i(\vec{k}_{\bar{1}}-\vec{k}_{\bar{1}}-\vec{p})\cdot\vec{R}_{n_0}}\,t_{n_0}(\vec{p})\,. \tag{A7}$$

By inspection of Eq. (A5) we see that the renormalization procedure for the inelastic processes resulted in factorizeable renormalized vertices for the elastic processes occurring prior to the loss events and vice versa, and a crystal-loss scattering amplitude.

The expression for the amplitude given by Eq. (A5) can be transformed into the form given in Eq. (22) with the definitions given by Eqs. (17) and (18) in the text, by performing the following set of operations.[19] Under the assumption that all the scattering sites in a given subplane[24] parallel to the surface are equivalent we can label a site both by the subplane in which it lies and by its position within the subplane. The site position becomes

$$\vec{R}_n=\vec{P}+\lambda\vec{a}+d\lambda\hat{z}\,, \tag{A8}$$

where $\lambda\vec{a}$ is the position of the origin in the λth subplane (to allow for a shift between successive subplanes),[6] $\vec{P}$ is the position of the site relative to the origin, and $d\lambda$ is the distance of the λth subplane below the surface (the $z=0$ plane). Substituting the expression for the site position given by Eq. (A8) into the expression for the amplitude of the "three-step" process given by Eq. (A5) and defining the subplane continuum normalization as

$$\sum_{\vec{P}}e^{-(\vec{k}_{2_\parallel}-\vec{k}_{1_\parallel})\cdot\vec{P}}=\frac{(2\pi)^2}{A}\sum_{\vec{g}}\delta(\vec{k}_{2_\parallel}-\vec{k}_{1_\parallel}-\vec{g})\,, \tag{A9}$$

where $\vec{g}$ is a vector in the two-dimensional reciprocal lattice of the subplane and A the area of a primitive unit cell of the subplane, we convert from sums over sites to sums over subplanes. The sums over sites parallel to the surface yield a δ-function conservation of the parallel components of the momenta parallel to the surface via Eq. (A9).

Grouping all sites lying in a given subplane together and using the definitions of the subplane-indexed scattering amplitudes given by the integral equations in Eqs. (17b) and (17c), we can write Eq. (A5) in the form given by Eq. (20) in the text, with the definition of $R(\vec{k}',\vec{k},E)$ given by Eq. (17a). The renormalization procedure for the generalized "two-step" inelastic processes follows in the same way. By substituting the expression for the scattering amplitudes into Eq. (23) we get the expression for the cross section. A further reduction of the formulas in which we transform them into a form amenable for numerical calculations[18] is described in Appendix B.

APPENDIX B

In this Appendix, we derive an expression for the inelastic cross section of an electron exciting a surface plasmon in the multiple-scattering treatment of ILEED.

The starting formulas are Eqs. (19)–(22) in the text. Let us first describe the evaluation of the "three-step" contribution to the differential cross section [Eq. (22) and Fig. (1e)]. Using the definitions of the quantities appearing in Eq. (22) given in Eqs. (17a) and (18) the sum over atomic sites parallel to the surface can be performed in a straightforward manner yielding

$$A_3'(\vec{k}',\vec{k},\vec{p},E,w)=\sum_{n\lambda_3}\sum_{\lambda_1,\lambda_2}\int\frac{d^3k_1}{(2\pi)^3}\int\frac{d^3k_2}{(2\pi)^3}\sum_{\vec{g}_1}\frac{(2\pi)^2}{A}\,\delta(\vec{k}_{1_\parallel}-\vec{k}_\parallel-\vec{g}_1)\,T_{\lambda_1}(E)\,(e^{-i(k_{1_\perp}-k_\perp)d}\,e^{-i\vec{g}\cdot\vec{a}})^{\lambda_1}$$
$$\times\left(-\frac{2m}{\hbar^2}\right)\frac{1}{k_1^2-k^2(E)}\left[\frac{2\pi m}{\hbar^2}\left(\frac{\pi e^2\hbar\omega_s\Omega^2}{p_\parallel}\right)^{1/2}e^{-i(\vec{k}_{2_\parallel}-\vec{k}_{1_\parallel}-\vec{p}_\parallel)\cdot\vec{R}_{n_\parallel}}\,e^{-i(k_{2_\perp}-k_{1_\perp})d\lambda_3}\,e^{-p_\parallel d|\lambda_3|}\left(-\frac{2m}{\hbar^2}\right)\frac{1}{k_2^2-k^2(E-w)}\right.$$

$$\times \sum_{\vec{g}_2} \frac{(2\pi)^2}{A}\,\delta(\vec{k}_{2\parallel}-\vec{k}'_{\parallel}+\vec{g}_2)\,T_{\lambda_2}(E-w)\,(e^{-i(k'_\perp-k_{2\perp})d}\,e^{-i\vec{g}\cdot\vec{a}})^{\lambda_2}\Big]\,. \quad \text{(B1)}$$

All symbols are defined in the text. The lattice sums parallel to the surface yield in an additional parallel momentum conservation relation (i.e., δ function)

$$\vec{k}'_{\parallel}=\vec{k}_{\parallel}+\vec{p}_{\parallel}+(\vec{g}_1+\vec{g}_2)\,. \quad \text{(B2)}$$

Equation (B2) is accompanied by the restriction on the intermediate-beam indices

$$\vec{g}_1+\vec{g}_2=\vec{g}\,. \quad \text{(B3)}$$

Performing the integral over the intermediate momenta, we obtain

$$A'_3(\vec{k}',\vec{k},\vec{p},E,w)=\sum_{\vec{g}_1,\vec{g}_2}\frac{(2\pi)^2}{A}\,\delta(\vec{k}'_{\parallel}-\vec{k}_{\parallel}-\vec{p}_{\parallel}-\vec{g}_1-\vec{g}_2)$$

$$\times\frac{2\pi m}{h^2}\left(\frac{\pi e^2\hbar\omega_s\Omega^2}{p_{\parallel}}\right)^{1/2}\left(\frac{mi}{\hbar^2 A k_\perp(\vec{g}_1,E-w)}\right)$$

$$\times\left(\frac{mi}{\hbar^2 A k_\perp(-\vec{g}_2,E-w)}\right)[S_3^a+S_3^b] \quad \text{(B4)}$$

in which S_3^a and S_3^b given by Eqs. (34) and (35) correspond to the two sets of layer sums mentioned in Sec. IV A. Assigning the layer index λ_3 to the layer at which a loss process occurs and λ_1, λ_2 to the layers at which multiple-elastic-diffraction processes occur before and after the loss process, respectively, the two sets of layer sums to be considered are (1) S_3^a, for which $\lambda_1<\lambda_3<\lambda_2$, i.e., the first elastic-multiple-scattering vertex occurs closer to the metal surface than the loss process, while the second one occurs deeper; (2) S_3^b, for which $\lambda_1>\lambda_3>\lambda_2$; i.e., the first elastic-multiple-scattering vertex lies further from the surface than the "loss-process layer," and the second one occurs closer to the surface. Processes in which λ_1, $\lambda_2>\lambda_3$ or $\lambda_3>\lambda_1$, λ_2 are not allowed because of the forward-scattering nature of the plasmon-emission vertices. Hence $\lambda_3>0$ always, and there are no contributions from the coupling to the surface plasmons outside the solid in the "three-step" diagram. However, this coupling contributes to the other two steps[8,9] [D-L and D-D, e.g., Figs. 1(c)–1(d)]. The evaluation of these other contributions proceeds along similar lines. In the case of bulk-plasmon excitation using a coherent electron-plasmon vertex[1] we substitute

$$t(p)\,e^{ip_\perp R_\perp}\to\left(\frac{\pi e^2\hbar\omega_b\Omega^2}{2p^2}\right)^{1/2}\frac{e^{ip_\perp R_\perp}-e^{-ip_\perp R_\perp}}{i} \quad \text{(B5)}$$

and

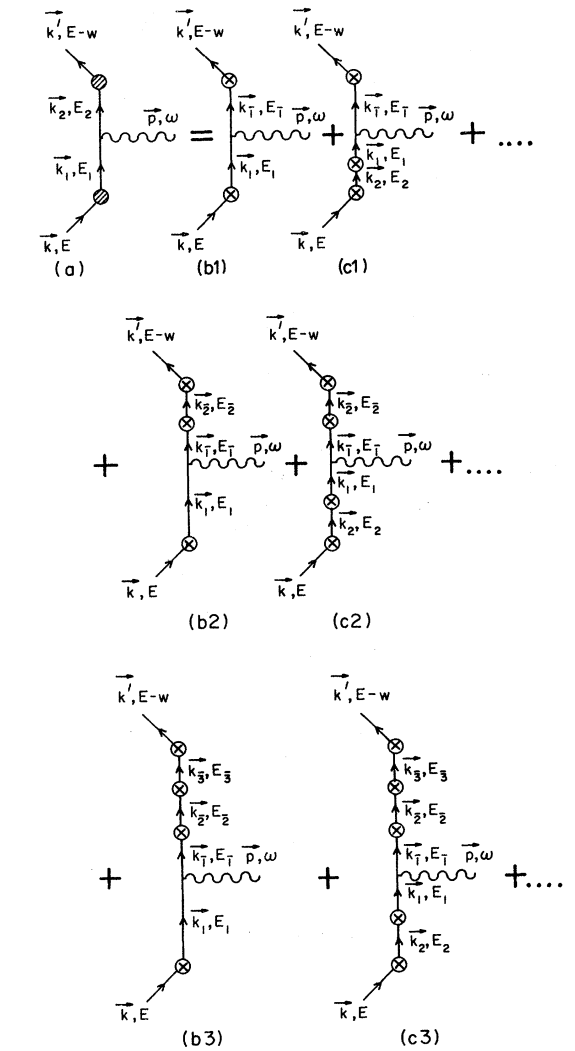

FIG. 4. A diagrammatic description of the renormalization procedure for the "three-step" process of multiple-elastic-diffraction processes before and after the loss event. (a) The renormalized "three-step" process; (b1) and (c1) diagrams contributing to step (1) in the renormalization procedure. Multiple-elastic-scattering events before the loss process and *one* elastic-scattering event after the loss; (b2) and (c2) diagrams contributing to step (2) in the renormalization procedure. Multiple-elastic-scattering events before the loss process and *two* elastic scattering events after the loss; (b3) and (c3) diagrams contributing to step (2) in the renormalization procedure. The perturbation-theory definition of the expressions for the cross sections associated with these diagrams is given by Duke and Laramore (Ref. 1). The shaded circle indicates the summation of an arbitrary number of individual elastic-scattering events (designated by the circled cross).

$$\sum dp_\perp \to \int_0^{P_{cb}} \frac{dp_\perp}{\pi} , \tag{B6}$$

in order to normalize to sine-wave rather than plane-wave basis functions. The final expressions for the cross sections are evaluated by assuming $\omega \gg \kappa T$ and taking for the surface plasmons

$$\mathrm{Im}D_s(\vec{p}_\parallel, w) = \Gamma_s(p_\parallel)/\{[w - \hbar\omega_s(p_\parallel)]^2 + [\Gamma_s(p_\parallel)]^2\} \tag{B7}$$

and

$$\mathrm{Im}D_b(\vec{p}, w) = \Gamma_b(\vec{p}_\parallel, p_\perp)/\{[w - \hbar\omega_b(\vec{p}_\parallel, p_\perp)]^2 + [\Gamma_b(\vec{p}_\parallel, p_\perp)]^2\} \tag{B8}$$

for the bulk. The calculations of the D-L and L-D amplitudes, A_1' and A_2' in Eq. (23), are outlined in the Appendix to Ref. 9. They are similar in our case, with the ion core t_λ replaced by the multiple-scattering vertices T_λ.

Finally it is worth noting that when the multiple-scattering amplitude T_λ is replaced by the layer-independent scattering amplitude t, the layer sums can be performed analytically. In this limit our expressions for the D-L and L-D contributions to the inelastic differential cross sections [Eqs. (30), (31), (37), and (38)] reduce to the corresponding ones derived by Bagchi and Duke.[9]

---

*Research sponsored in part by the Air Force Office of Scientific Research, Office of Aerospace Research, USAF, under Grant No. AFOSR 71-2034. The United States Government is authorized to reproduce and distribute reprints for governmental purposes notwithstanding any copyright notation hereon.

†Present address: Xerox Research Labs., Xerox Square, Rochester, N. Y. 14644.

[1]C. B. Duke and G. E. Laramore, Phys. Rev. B 3, 3183 (1971).

[2]G. E. Laramore and C. B. Duke, Phys. Rev. B 3, 3198 (1971).

[3]C. Davisson and L. H. Germer, Phys. Rev. 30, 705 (1927).

[4]J. C. Turnbull and H. E. Farnsworth, Phys. Rev. 54, 507 (1938).

[5]P. P. Reichertz and H. E. Farnsworth, Phys. Rev. 75, 1902 (1949).

[6]C. B. Duke, J. R. Anderson, and C. W. Tucker, Jr., Surface Sci. 19, 117 (1970).

[7]C. B. Duke, A. J. Howsmon, and G. E. Laramore, J. Vac. Sci. Technol. 8, 10 (1971).

[8]C. B. Duke and A. Bagchi, J. Vac. Sci. Technol. 9, 738 (1972).

[9]A. Bagchi and C. B. Duke, Phys. Rev. B 5, 2784 (1972).

[10]C. B. Duke, G. E. Laramore, and V. Metze, Solid State Commun. 8, 1189 (1970).

[11]A. Bagchi, C. B. Duke, P. J. Feibelman, and J. O. Porteus, Phys. Rev. Letters 27, 998 (1971).

[12]C. W. Tucker, Jr. and C. B. Duke, Surface Sci. 24, 31 (1971).

[13]G. Capart, Surface Sci. 26, 429 (1971).

[14]D. W. Jepsen, P. M. Marcus, and F. Jona, Phys. Rev. Letters 26, 1365 (1971).

[15]J. B. Pendry, J. Phys. C 4, 2514 (1971).

[16]G. E. Laramore, C. B. Duke, A. Bagchi, and A. B. Kunz, Phys. Rev. B 4, 2058 (1971).

[17]G. E. Laramore and C. B. Duke, Phys. Rev. B 5, 267 (1972).

[18]C. B. Duke and U. Landman, following paper, Phys. Rev. B 6, 2968 (1972).

[19]C. B. Duke and G. E. Laramore, Phys. Rev. B 2, 4765 (1970); 2, 4783 (1970).

[20]P. J. Feibelman, C. B. Duke, and A. Bagchi, Phys. Rev. B 5, 2436 (1972).

[21]J. I. Gersten, Phys. Rev. 188, 774 (1969).

[22]H. Raether, Ergeb. Exakt. Naturw. 38, 84 (1965).

[23]C. B. Duke, and C. W. Tucker, Jr., Surface Sci. 15, 751 (1969).

[24]J. L. Beeby, J. Phys. C 1, 82 (1968).

[25]C. B. Duke, D. L. Smith, and B. W. Holland, Phys. Rev. B 5, 3358 (1972).